The Osmium Isotope Signature of Phanerozoic Large Igneous Provinces

Book Section

Part III
Geochemical Proxies for the Environmental Effects of LIPs

10

The Osmium Isotope Signature of Phanerozoic Large Igneous Provinces

Alexander J. Dickson[1], Anthony S. Cohen[2], and Marc Davies[3]

ABSTRACT

The emplacement of Large Igneous Provinces (LIPs) throughout the Phanerozoic Eon introduced vast quantities of mafic rocks to the Earth's surface, which were subsequently weathered into the oceans. Osmium isotope data can be used to track these LIP-related weathering fluxes, providing a global fingerprint of the timing and magnitude of LIP emplacement, and guiding assessments of the impact of these events on ocean biogeochemistry and the regulation of the global climate system. Sedimentary Os isotope records spanning late Phanerozoic LIP events are reviewed herein and new observations from Eocene hyperthermal event ETM-2 are presented. While Os isotope stratigraphy can provide major constraints on LIP activity in the geological record, it cannot always distinguish whether the extrusive activity was subaerial or submarine. The utility of osmium isotopes as a global tracer of past volcanism may be enhanced when used alongside proxies such as mercury concentrations, which may be more diagnostic of the style of individual episodes of LIP emplacement. Hitherto, only a few high-resolution Os-isotope records across Phanerozoic LIPs have effectively exploited the short oceanic residence time of Os. Future high-resolution studies across suitable, well-preserved stratigraphic records will significantly improve our understanding of the nature, progression, and consequences of LIP emplacement.

10.1. INTRODUCTION

The emplacement of Large Igneous Provinces (LIP) is characterized by anomalously high magmatic fluxes, such that the majority of their volume is emplaced within a relatively short time-period of <1–2 million years. They comprise massive volumes of mantle-derived igneous material sometimes in excess of 10^6 km^3, intruded into the crust as dykes, sills, and batholiths, and extruded onto the surface as effusive lava flows or as explosive ejecta together with a cocktail of superheated gases and fluids in either a subaerial or submarine environment (Coffin & Eldholm, 1992, 1994; Ernst, 2014). LIPs have often been linked to mantle plumes, which are persistent upwellings of anomalously hot mantle. The rapid eruption rates and huge volumes of material sourced from melting in the plume head during the early stages of LIP emplacement far exceed present-day eruption rates and volumes, and because of this rapidity they are proposed to have had a deleterious impact on the global environment. LIPs occurred periodically throughout Earth's history, at approximate intervals of a few tens of millions of years (Prokoph et al., 2013) and have been associated with episodes of extreme global climate change and biotic extinction (Ernst & Youbi, 2017; Bond & Sun, Chapter 3 this volume; Ernst et al., Chapter 1 this volume) (Fig. 10.1).

Several key questions regarding LIP behavior have been postulated: When did individual LIP events occur? Was volcanic activity continuous or intermittent over the period of emplacement? Did LIP emplacement drive

[1]*Department of Earth Sciences, Royal Holloway University of London, Egham, United Kingdom*

[2]*Department of Environment, Earth and Ecosystems, The Open University, Milton Keynes, United Kingdom*

[3]*School of Geography, Earth and Environmental Sciences, University of Plymouth, Plymouth, United Kingdom*

Large Igneous Provinces: A Driver of Global Environmental and Biotic Changes, Geophysical Monograph 255, First Edition.
Edited by Richard E. Ernst, Alexander J. Dickson, and Andrey Bekker.

DOI: 10.1002/9781119507444.ch10

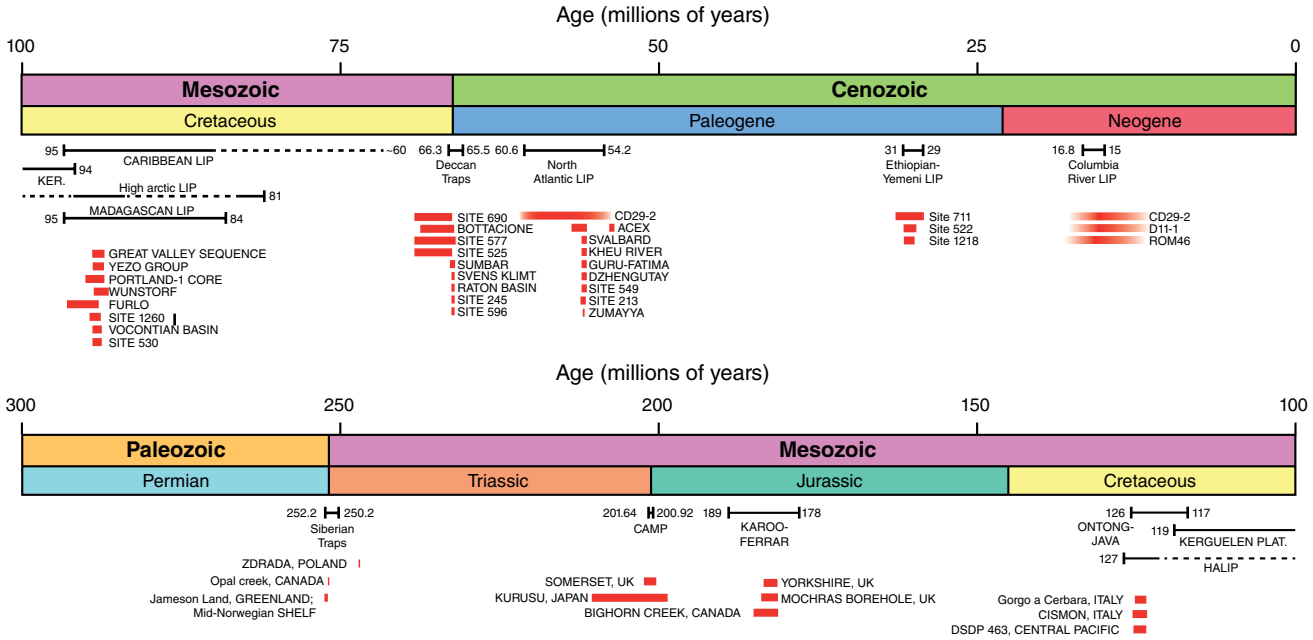

Figure 10.1 Ages of Late Phanerozoic LIPs and the temporal overlap of existing $^{187}Os/^{188}Os_{(i)}$ records with these volcanic events. Ages for each LIP are taken from Barry et al. (2013), Schoene et al. (2015), Duncan et al. (1997), Hofmann et al. (1997), Duncan (2002), Storey et al. (2007), Timm et al. (2011), Blackburn et al. (2013), Loewen et al. (2013), Burgess and Bowring (2015), Davies et al. (2017), and Kingsbury et al. (2018). Dashed lines indicate approximate periods of reduced activity within the overall duration of a LIP.

changes in the global climate system? What climatic feedback processes do LIPs perturb? Do all LIPs alter Earth system processes (weathering, ocean chemistry, warming, etc.) in the same way? Do all LIPs cause biotic extinctions? The approach to answering many of these questions is commonly to undertake rigorous radiometric dating of igneous rocks that can be related to specific episodes of LIP activity. These efforts initially centered on Ar-Ar dating of flood basalts. These Ar-dating approaches have been instrumental in establishing first-order relationships between the timing of LIP events and major extinction and environmental changes across the Phanerozoic and beyond (Wignall et al., 2001), but are sometimes limited by relatively large absolute age uncertainties, which may be on the order of ~ $\pm 10^5$–10^6 years. Recent advances in U-Pb dating, with reported age uncertainties of $\pm 10^4$ years, have significantly reduced the age uncertainties on some LIP events, thereby allowing a greater understanding of how individual episodes of LIP activity may proceed within a longer period of emplacement (e.g., Schoene et al., 2010; Svensen et al., 2010; Blackburn et al., 2013; Burgess & Bowring, 2015; Davies et al., 2017; other contributions in this volume). Ultra-high-resolution dating of magmatic episodes has greatly improved our understanding of the nature of LIP activity, providing a precise framework to explore the potential of volcanic activity as a trigger for the complex environmental changes and feedbacks leading to mass extinction events. Nonetheless, this approach requires the preservation of datable rocks that can be stratigraphically related to the overall LIP sequence. This requirement inevitably leads to LIP chronologies that can potentially be discontinuous and patchy.

Despite these limitations, recent advances in radiometric dating have shown that the catastrophic environmental changes potentially driven by LIP volcanism are triggered by intense short-lived volcanic episodes rather than persistent volcanism spanning the entire period of emplacement. Similarly, the associated feedback processes set in motion (including carbon cycle reorganization, climatic warming, weathering, ocean anoxia, and biotic extinction) operate on comparable centennial-millennial timescales. Therefore, in order to constrain the magnitude and duration of these perturbations and establish an order of events, it is necessary to generate proxy data with age constraints precise enough to resolve the environmental changes in the stratigraphic record. Strontium isotopes have been used to constrain the source and duration of weathering during extended warming events, but the long oceanic residence time of Sr (>4 million years; Veizer, 1989) limits its ability to resolve very short-term weathering events. The very much shorter ocean residence time of Os (~10–50 Kyr; Sharma et al., 1997; Levasseur et al., 1999) makes its isotope system a more effective tracer of relatively rapid changes in the temporal evolution of global seawater chemistry as it

continually adjusts to the input of Os weathered from newly emplaced volcanic rocks. This feature gives Os-isotope stratigraphy the almost unique quality of being able to trace the temporal progression of LIP events at fine levels of detail (potentially $<10^4$ years) at far-field sites that are not affected by the erosion or thermal alteration processes that can disturb sedimentary successions in more proximal settings. It is this utility of Os isotopes that will form the focus of this contribution.

10.2. OS ISOTOPE STRATIGRAPHY

Rhenium and Os readily partition into metal, sulfide, and organic phases, and because of this behavior the Re-Os isotope system provides a complementary record of geological processes compared with silicate-hosted isotopic systems such as Rb-Sr, Sm-Nd, Lu-Hf, and U-Pb. Rhenium and Os show differences in compatibility, which give rise to contrasting low and high Re/Os ratios for the mantle and crust, respectively. This marked parent-daughter fractionation and the subsequent radiogenic ingrowth of ^{187}Os as a result of β-decay of ^{187}Re produces orders of magnitude variations in the ^{187}Os/^{188}Os of geological reservoirs. In crustal rocks, where the Re/Os ratio is relatively high, the in-situ production of ^{187}Os leads to high (radiogenic) ^{187}Os/^{188}Os ratios that average ~1.4 (Peucker-Ehrenbrink & Jahn, 2001). In mantle and ultramafic rocks, where Re/Os ratios are low, ^{187}Os/^{188}Os ratios are lower (unradiogenic) with a value that is more chondritic in nature, ~0.12 (Luck & Allègre, 1983). The oceans record the proportional mixing of the two Os isotope end-members (Peucker-Ehrenbrink & Ravizza, 2000) (Fig. 10.2).

Three important aspects of the Os-isotope system in regard to LIPs need to be considered. First, Os isotopes are an indirect tracer for LIP activity. The rapid emplacement of LIPs can result in the intense and rapid weathering of juvenile mafic and ultramafic rocks, either by atmospheric and biogeochemical processes, low-temperature submarine basalt-seawater interaction, or creation of hydrothermal systems around submarine volcanic centers (Peucker-Ehrenbrink & Ravizza, 2000; Cohen & Coe, 2002; Turgeon & Creaser, 2008). These weathering fluxes release unradiogenic Os into seawater, which lowers the seawater ^{187}Os/^{188}Os ratio. However, if LIP rocks are not easily susceptible to weathering, or if LIP activity remobilizes Os from previously buried sedimentary reservoirs, the ^{187}Os/^{188}Os ratio of seawater might instead record a shift toward radiogenic values. This trend may be amplified if climate feedbacks associated with widespread volcanism are able to increase the congruency of terrestrial rock weathering. In practice, the Os-isotope

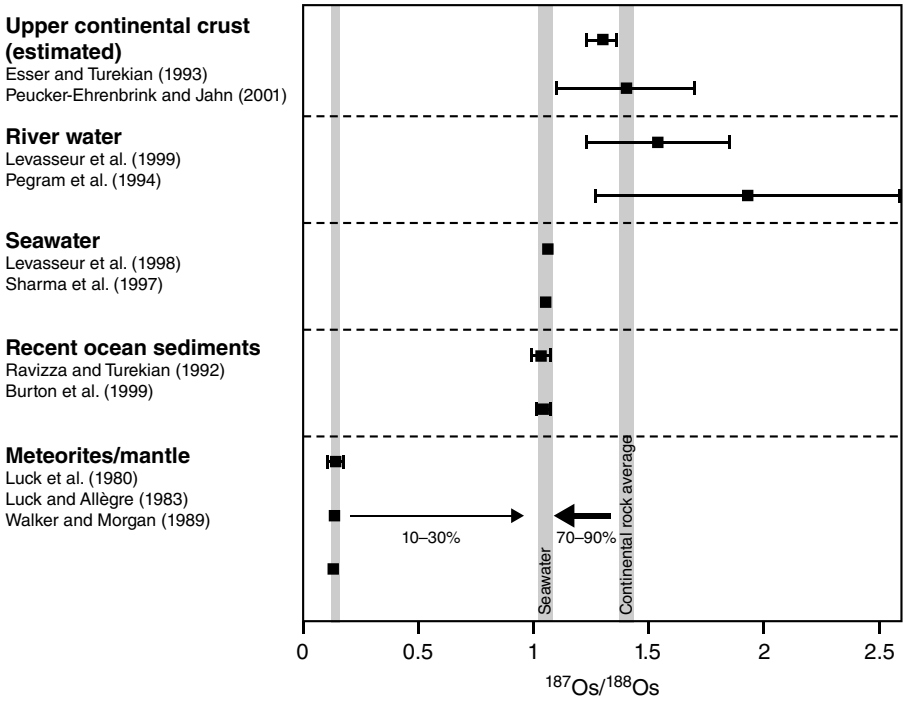

Figure 10.2 The modern mass balance of osmium. Osmium isotope ratios for different geological materials are shown along with key literature references. The modern seawater value of ~1.06 represents a contribution of ~10% to 30% from unradiogenic (mantle and extraterrestrial dust) fluxes and ~70% to 90% from radiogenic sources in the continental crust.

"signature" of a LIP might involve swings in seawater $^{187}Os/^{188}Os$ in either direction at different times, a feature that is clearly apparent during many LIP events, for example, the Ontong-Java Plateau and the North Atlantic Igneous Province (Bottini et al., 2012; Dickson et al., 2015). The second important feature of the Os isotope system is the short residence time of Os in the oceans, of ~10–50 kyrs (Sharma et al., 1997; Levasseur et al., 1999). This feature provides Os-isotope stratigraphy with the potential for tracing the pulsed emplacement of LIPs at timescales of 10^3–10^4 years, and the nature of the associated climate/weathering feedbacks. As will be discussed, this utility has rarely been fully exploited for any individual LIP to date. Finally, the Os-isotope composition of the oceans can also be influenced by extraterrestrial fluxes, such as from impactor events (e.g., Sato et al., 2013) or cosmogenic particles (Ravizza, 2007). Extraterrestrial impacts have been suggested for several intervals bracketed by LIPs, and these must be borne in mind when examining the reconstructed temporal evolution of seawater chemistry.

Osmium is present in seawater only in ultra-trace concentrations but is strongly enriched in reducing marine sediments. The enrichment of Os (and Re) in low-oxygen depositional settings means that paleo-seawater $^{187}Os/^{188}Os$ ratios can be traced by the careful measurement of Re and Os compositions in organic-rich mudrocks, followed by a correction for the postdepositional decay of ^{187}Re (Ravizza & Turekian, 1989, 1992; Cohen et al., 1999). The requirement to correct $^{187}Os/^{188}Os$ ratios in organic-rich rocks for ^{187}Re decay means that so-called initial Os-isotope stratigraphies (Os_i) have been produced mainly for those events where suitable deposits exist with independent age control. Where there is no independent age control, "initial" $^{187}Os/^{188}Os$ ratios can be estimated using the isochron approach of measuring samples with different $^{187}Re/^{188}Os$ ratios collected from a restricted stratigraphic range (e.g., Cohen et al., 1999). Some Os-isotope records have also been produced from Fe-Mn crusts and oxic metalliferous sediments (e.g., Pegram et al., 1992; Peucker-Ehrenbrink et al., 1995; Burton et al., 1999; Ravizza et al., 2001; Klemm et al., 2005, 2008; Burton, 2006; Robinson et al., 2009). These records do not require a significant correction for Re decay, but may be systematically biased due to the partial liberation of detritally hosted Os phases from the bulk sediment (e.g., Pegram & Turekian, 1999). Furthermore, such records from Fe-Mn crusts have a limited temporal resolution because of their slow accumulation rates. In all types of approach (mudrocks or crusts/sediments), Os_i records spanning early Phanerozoic LIPs (i.e., pre-Permian) have not yet been widely produced. The LIP record of only the late Phanerozoic will therefore be summarized in the following discussion and illustrated in Figures 10.3 and 10.4.

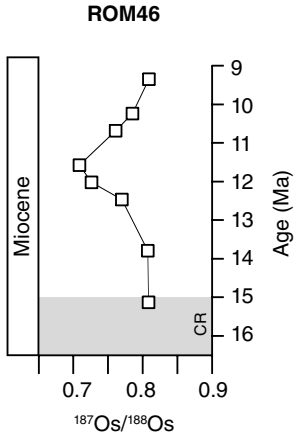

Figure 10.3 Miocene Os-isotope data spanning the emplacement of the Columbia River LIP. Data are from Klemm et al. (2008). The grey-shaded region denotes a shift toward more unradiogenic seawater $^{187}Os/^{188}Os$ ratios that are taken to record the rapid weathering of basalts associated with LIP emplacement and/or a reduction in the weathering rate of continental rocks.

10.3. THE PHANEROZOIC OS-ISOTOPE RECORD OF LIPS

10.3.1. The Columbia River LIP (~17–15 Ma)

As the youngest LIP of the Phanerozoic, the Columbia River (CR) event has a very well defined chronology and stratigraphic framework (Barry et al., 2013; Riedel et al., 2013). $^{40}Ar/^{39}Ar$ and K-Ar age determinations of the CR eruptive history suggested that activity occurred across a total interval of ~16.9–6 Ma, with most activity occurring during emplacement of the Grande Ronde basalt, from ~16–15.6 Ma (Barry et al., 2013). Recent zircon U-Pb ages of CR ashes have refined this chronology to constrain ~95% of the eruptive history to the interval 16.7–15.9 Ma (Kasbohn & Schoene, 2018). There are few Os-isotope data that record the impact of the CR LIP on ocean chemistry. The records that exist are from oceanic ferromanganese crusts, which record changes in seawater $^{187}Os/^{188}Os$ at multimillion-year timescales that are far in excess of the oceanic residence time of Os (Klemm et al., 2005, 2008; Burton, 2006). These records (illustrated in Fig. 10.3) do suggest a small $^{187}Os/^{188}Os$ shift of ~0.1 toward more unradiogenic ratios in seawater during the Miocene, as would be expected from an enhanced weathering flux of unradiogenic Os from CR basalts (Klemm et al., 2008). However, the timing of this shift depends on the age-model applied to the crust records. Even revised age-models based on Os-isotope stratigraphy imply an unradiogenic shift in $^{187}Os/^{188}Os$ between ~15 and 12 Ma, a pattern that significantly postdates radiometric ages of most of the CR eruptive episodes. For a LIP to have had a discernable impact on Os ocean chemistry, it must have

been volumetrically large, the constituent lavas and intrusive rocks must have contained high Os concentrations, and the rocks must have been weathered rapidly following emplacement. Although effusion rates in individual pulses of CR volcanism may have been comparable to larger LIPs in the geological record, the CR river event was volumetrically small compared with many earlier Phanerozoic LIPs, and the amount of basalt weathered was orders of magnitude smaller than, for example, the CAMP event at the Triassic-Jurassic boundary (Cohen & Coe, 2002). Thus, it is possible that the putative unradiogenic signal observed by Klemm et al. (2008) is actually unrelated to the CR LIP, and records a different perturbation to Os ocean chemistry in the Miocene.

10.3.2. Ethiopian-Yemeni Flood Basalts (~31–29 Ma)

The Ethiopian-Yemeni LIP has the best-preserved sequence of flood basalts in the Cenozoic geological record. The main phase of flood basalt volcanism began shortly before ~30 Ma and lasted for less than ~1 million years (Hofmann et al., 1997; Ukstins et al., 2002) before continuing in pulses concomitant with the opening of the Red Sea and the Gulf of Aden (Courtillot & Renne, 2003). Magnetostratigraphy of the Ethiopian flood basalts indicates a correlation to magnetochrons C11r to C11n (Hofmann et al., 1997; Touchard et al., 2003), making them younger than the Eocene-Oligocene boundary event, which occurred during chrons C13r–C12r (~34 Ma; e.g., Zachos et al., 1996). The effect of the Ethiopian-Yemeni LIP on the osmium chemistry of the oceans is not well understood, with low-resolution data available from only three locations (Peucker-Ehrenbrink & Ravizza, 2012). These records agree in the sense that they all show $^{187}Os/^{188}Os$ ratios evolving to less radiogenic values at ~30–31 Ma. However, the magnitude and pattern of this decrease varies, from ~0.08 in Indian Ocean ODP Site 711, to ~0.12 in South Atlantic DSDP Site 522 (Peucker Ehrenbrink & Ravizza, 2012). Os-isotope stratigraphy therefore appears to reveal a signature of basalt weathering on ocean chemistry, though the true size of this weathering flux and its wider temporal context are limited by the available data.

10.3.3. The North Atlantic Igneous Province (NAIP) (~61–54 Ma)

The emplacement of the NAIP near the Paleocene-Eocene boundary has been suggested to have influenced the genesis of rapid global warming during the Paleocene-Eocene Thermal Maximum (PETM; Storey et al., 2007; Frieling et al., 2016), an event that also includes an extinction of benthic foraminifera (Thomas & Shackleton, 1996). The NAIP consists of a series of subaerial lava flows and intrusive units (e.g., Svensen et al., 2004, 2010) that are dated to between ~60 and ~53 Ma (Storey et al., 2007; Svensen et al., 2010; Wilkinson et al., 2017). Only two existing Os-isotope records (from Fe-Mn crusts CD-29 and D11-1) cover the entire period of emplacement (Klemm et al., 2005; Burton, 2006). These records show a shift in seawater $^{187}Os/^{188}Os$ to slightly more unradiogenic values, as would be expected as extruded basalts began to weather into the oceans (Fig. 10.4). A number of high-resolution Os-isotope records span the Paleocene-Eocene boundary (Ravizza et al., 2001; Weiczorek et al., 2013; Dickson et al., 2015), when the accumulation rate of NAIP basalts increased significantly at the commencement of seafloor spreading (Storey et al., 2007b). These records actually show a small change (~0.05) to more radiogenic $^{187}Os/^{188}Os$ ratios that has been interpreted to reflect enhanced weathering of terrestrial rocks due to elevated atmospheric temperatures and moisture (Ravizza et al., 2001; Dickson et al. 2015). The small magnitude of the increase in $^{187}Os/^{188}Os$ compared with other Phanerozoic events (e.g., Cohen et al., 2004) may be due to the competing influences of Os being weathered from both radiogenic and unradiogenic sources at the same time. Several of the NAIP data sets also demonstrate a very brief shift to more unradiogenic values in seawater near the Paleocene-Eocene boundary, which likely records a pulse of unradiogenic Os associated with magmatic activity at the commencement of the PETM (Weiczorek et al., 2013; Dickson et al., 2015), or perhaps an extraterrestrial impact event (c.f. Schaller et al., 2017). The stratigraphic correspondence between unradiogenic Os-isotope ratios and a peak in Hg concentrations in pre-PETM deposits in Svalbard tend to support a volcanic origin for this feature (Jones et al., 2019). This observation highlights the potential for Os isotope stratigraphy to reveal very fine-scale detail of volcanic activity that is pertinent to testing hypotheses relating LIP emplacement to rapid climate change.

The influence of episodic NAIP activity on brief global warming events (hyperthermals) that occurred *after* the PETM is largely untested. A new Os-isotope record is shown in Figure 10.4 (data in Table 10.1) from IODP Site M0004A (Arctic Ocean) spanning one such event, Eocene Thermal Maximum 2 (~53 Ma). These data were produced using techniques identical to those of Dickson et al. (2015). Initial Os-isotope ratios increase by ~0.1 (0.38–0.48) shortly before the carbon isotope excursion that marks the start of the event, and again in more dramatic fashion at the termination of the carbon cycle perturbation, from ~0.4 to 0.8. The data are similar to $^{187}Os/^{188}Os$ ratios of metalliferous sediments from DSDP 549 that contain a shift to more radiogenic values (from ~0.44 to 0.50) across ETM 2 (Peucker-Ehrenbrink & Ravizza, 2012), thus supporting the hypothesis of a rapid increase in continental weathering across the hyperthermal. A single unradiogenic value of 0.18 also stratigraphically precedes ETM 2 at Site

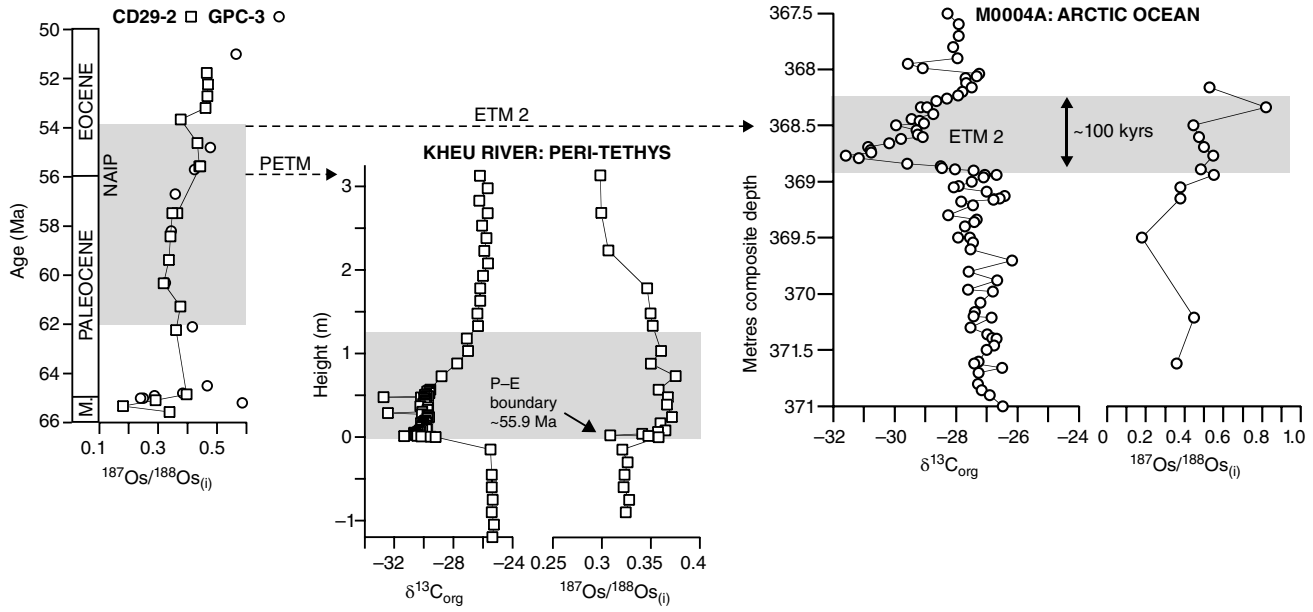

Figure 10.4 Paleocene-Eocene Os-isotope data spanning the emplacement of the North Atlantic Igneous Province. Fe-Mn crust data are from Klemm et al. (2005); all PETM data are from Dickson et al. (2015); ETM-2 Os isotope data are presented in this paper; ETM-2 C-isotope data for IODP Site M0004A are compiled from Sluijs et al. (2009) and Dickson and Cohen (2012). Grey-shaded regions denote the main phases of the PETM and ETM-2.

Table 10.1 Osmium data for IODP Site M0004A

Sample (core-section-top depth-lower depth)	Depth (mcd)	Os (pg/g)	Re (ng/g)	$^{187}Re/^{188}Os$	$^{187}Os/^{188}Os$	±	$^{187}Os/^{188}Osi$
27-1-76-77	368.16	280.6	65.2	1354.76	1.741	0.002	0.529
27-1-94-95	368.34	671.4	359.3	4021.20	4.419	0.017	0.820
27-1-110-111	368.50	641.1	161.2	1468.63	1.759	0.003	0.444
27-1 (120-121)	368.60	330.4	76.3	1335.92	1.670	0.002	0.475
27-1-129-130	368.69	523.7	99.7	1076.04	1.463	0.004	0.500
27-1-137-138	368.77	428.7	147.8	2171.30	2.490	0.005	0.546
27-1-149-150	368.89	514.7	116.3	1304.16	1.650	0.003	0.483
27-2-4-5	368.94	213.5	15.7	389.80	0.901	0.002	0.552
27-2-15-16	369.05	630.8	215.0	2096.88	2.256	0.003	0.379
27-2-25-26	369.15	180.0	31.8	974.19	1.250	0.001	0.378
27-2-60-61	369.50	370.1	87.6	1324.71	1.366	0.002	0.180
27-2-131-132	370.21	261.8	25.3	512.49	0.906	0.002	0.447
27-3-22-23	370.62	334.4	67.6	1130.95	1.370	0.001	0.358

M0004A (Fig. 10.4). Given the short duration of the ETM 2 (~100 kyrs) the unradiogenic value before the event began is at least consistent with a volcanic trigger. These observations come with the caveat of increasing hydrographic restriction in the Arctic during the Early Eocene (Brinkhuis et al., 2006; Dickson et al., 2015) that may have caused the $^{187}Os/^{188}Os$ ratio of Arctic Ocean seawater to deviate from the global value, although the comparison of ETM 2 data from Site M0004A and Site 549 suggest that this effect was small. The NAIP is a clear candidate for future high-resolution Os-isotope studies that seek to unravel the interaction of volcanism and climate change in the early Cenozoic.

10.3.4. The Deccan Traps (~66.3–65.5 Ma)

Ar-Ar age estimates of the timing of LIP emplacement place the Deccan Traps close to the mass-extinction event at the Cretaceous-Paleogene boundary (K-Pg)

(Chenet et al., 2007). U-Pb dating of zircons recovered from ashfall and erosive units interbedded with lava flows has recently allowed the chronology of this event to be improved substantially, with an estimate of ~753 kyrs for 80%–90% of the total eruptive history (Schoene et al., 2015). Os-isotope records from a variety of carbonate successions show reproducible trends in seawater $^{187}Os/^{188}Os$ prior to the K-Pg, with a ~20%–25% decrease toward unradiogenic values commencing at the C29r/C30n boundary, followed by a second decrease toward even more unradiogenic values occurring much closer to the K-Pg itself (Fig. 10.5; Ravizza & Peucker-Ehrenbrink, 2003; Robinson et al., 2009). Os data from K-Pg locations in Europe and the United States show that seawater $^{187}Os/^{188}Os$ decreased nearly to mantle values of ~0.14 at the acme of the unradiogenic shift prior to the K-Pg. This decrease is consistent both with an extraterrestrial impactor (Luck & Allègre, 1983; Esser & Turekian, 1989; Geissbühler, 1990; Peucker-Ehrenbrink et al., 1995; Meisel et al., 1995; Yin et al., 1995), and also with the emplacement of the Poldapur Deccan basalts, according to recent U-Pb data (Schoene et al., 2019). Osmium isotope data from latest Cretaceous rocks have been instrumental in testing the hypothesis that the eruption of the Deccan Traps caused the end-Cretaceous mass extinction. The earliest shift in $^{187}Os/^{188}Os$ associated with volcanism occurs considerably earlier than the major extinction horizon, an observation that tends to favor an extraterrestrial impactor as the cause of most (though not all) of the major biotic consequences of this time interval (Ravizza & Peucker-Ehrenbrink, 2003).

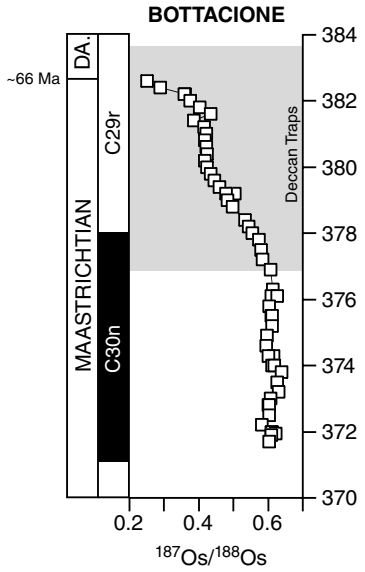

Figure 10.5 Maastrichtian-Paleocene Os-isotope data spanning the emplacement of the Deccan Traps and the K-Pg boundary. Data are from Robinson et al. (2009). The grey-shaded region denotes a shift toward more unradiogenic seawater $^{187}Os/^{188}Os$ ratios that are taken to record the rapid weathering of basalts associated with LIP emplacement and/or a reduction in the weathering rate of continental rocks.

The Deccan Traps illustrate an interesting conundrum in the interpretation of $^{187}Os/^{188}Os$ data in terms of LIP activity. Ravizza and Peucker-Ehrenbrink (2003) interpreted the decrease in $^{187}Os/^{188}Os$ commencing at the C29r/C30n boundary as recording a decrease in the weathering of radiogenic Os as flood basalts were extruded across crystalline basement rocks in the early phases of the Deccan LIP. This argument was in part supported by the low concentration of Os in Deccan basalts (Allègre et al., 1999). Other LIP events featuring a decrease in the $^{187}Os/^{188}Os$ of seawater have been interpreted in terms of an increase in the weathering of unradiogenic Os from mafic rocks (Turgeon & Creaser, 2008; Tejada et al., 2009; Bottini et al., 2012; Du Vivier et al., 2014). These differences highlight the fact that the marine $^{187}Os/^{188}Os$ ratio is the product of two competing inputs, and that the use of complementary data sets is often required to arrive at a satisfactory interpretation of the observed chemostratigraphic variations.

10.3.5. The Caribbean (~95–60 Ma), High Arctic (127–81 Ma), and Madagascan (~84–95 Ma) LIPs

Volcanism has long been hypothesized as a trigger for one of the most profound episodes of Phanerozoic ocean deoxygenation, at the Cenomanian-Turonian boundary. This event, Oceanic Anoxic Event 2 (OAE 2), took place at a similar time as the emplacement of several LIPs, most notably the Caribbean LIP (CLIP) and the High Arctic LIP (HALIP). Early studies attributed concentration spikes of mafic-derived trace elements in sedimentary rocks to infer volcanism (e.g., Orth et al., 1993), and this approach has continued recently (Eldrett et al., 2014). The publication of the first Os-isotope records for the Cenomanian-Turonian boundary, by Turgeon and Creaser (2008), revealed mantle-like signatures in global seawater that were sustained for hundreds of thousands of years during the acme of the environmental changes associated with OAE 2. These data firmly supported the significant role of voluminous volcanic activity in driving and sustaining widespread environmental change during this event, presumably through volcanism-climate feedbacks. Such feedbacks may have included the delivery of biolimiting nutrients and sulfate to the oceans, stimulating organic matter production and the consequent consumption of dissolved oxygen in many parts of the oceans (Adams et al., 2010; Jenkyns, 2010). The Os-isotope data sets of Turgeon and Creaser (2008) have since been supplemented by Du Vivier et al. (2014, 2015), who were able to show how abrupt shifts in $^{187}Os/^{188}Os_{(i)}$ ratios toward

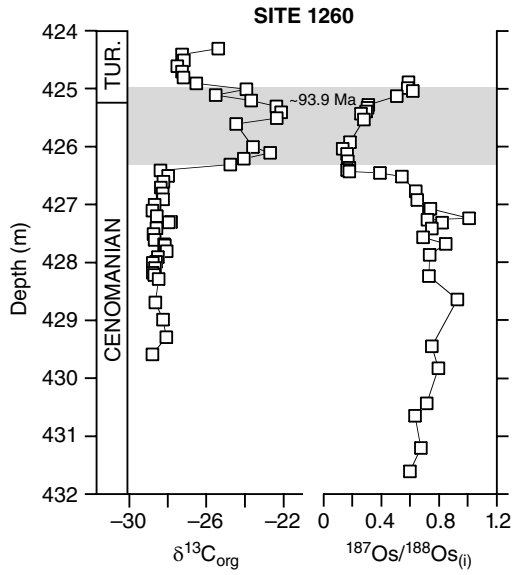

Figure 10.6 Cenomanian-Turonian Os-isotope data spanning Oceanic Anoxic Event 2, and a putative magmatic episode linked to the Caribbean LIP and/or the High Arctic LIP. C-isotope data are from Erbacher et al. (2005) and Os-isotope data are from Turgeon and Creaser (2008). The grey-shaded region denotes a shift toward more unradiogenic seawater $^{187}Os/^{188}Os$ ratios that are taken to record the rapid weathering of basalts associated with LIP emplacement and/or a reduction in the weathering rate of continental rocks.

mantle values (~0.15) occurred several thousands of years in advance of the positive carbon isotope excursion that defines the event (c.f. Tsikos et al., 2004) (Fig. 10.6). The persistence of unradiogenic Os-isotope values over a period of several hundreds of thousands of years, far in excess of the Os residence time in the oceans, demonstrates the prolonged period of time during which Os was weathered from volcanic rocks on land and/or by submarine basalt-seawater interaction (Turgeon & Creaser, 2008; Du Vivier et al., 2014, 2015). Furthermore, changes in the concentration of Os in sedimentary successions throughout the phase of otherwise unradiogenic Os-isotope ratios within OAE 2 may suggest small changes in the amount of Os being weathering into the oceans (Du Vivier et al., 2014, 2015). However, despite the clear signature of LIP activity afforded by the unradiogenic Os-isotope values that span OAE 2, these data are not able to unambiguously fingerprint the source of the unradiogenic Os flux. Various studies continue to debate the relative importance of volcanism associated with the HALIP (Eldrett et al., 2017) and the CLIP (Kuroda et al., 2007; Holmden et al., 2016; Scaife et al., 2017), while Ar-Ar ages for eruptive events associated with the Madagascan LIP (Cucciniello et al., 2010) also slightly overlap the age of the Cenomanian-Turonian boundary (Meyers et al., 2012). It is possible that these events all contributed in some way to the widespread environmental changes that occurred during OAE 2.

OAE 2 provides an interesting case study of hysteresis in Earth-system processes. The lead-lag relationship between Os-isotope and C-isotope changes at the onset of OAE 2 clearly supports the contention of a volcanic trigger with the rapid emplacement of submarine basalts, probably associated with the CLIP, being rapidly weathered into seawater. However, the shift to more radiogenic Os-isotope ratios in marine sediments before the end of OAE 2 does not clearly link to a decrease in global temperatures, as would be expected if volcanic CO_2 emissions slowed and were further reduced by silicate weathering and organic-carbon burial feedbacks (Robinson et al., 2019). As well as driving transient environmental changes, LIP volcanism may also drive Earth's climate system into new, quasi-stable states.

10.3.6. The Ontong-Java Plateau (~126–117 Ma)

Os-isotope stratigraphy has been instrumental in demonstrating that the emplacement of the Ontong-Java LIP in the ancestral Pacific Ocean occurred at precisely the same time as an episode of major environmental change, during Oceanic Anoxic Event 1a (Tejada et al., 2009; Bottini et al., 2012). These Os-isotope records, from locations in two different ocean basins, have strikingly similar $^{187}Os/^{188}Os_{(i)}$ values, and exhibit near-identical shifts in $^{187}Os/^{188}Os_{(i)}$ ratios when compared with the carbon- and bio-stratigraphic frameworks for each locality (Malinverno et al., 2010) (example in Fig. 10.7). The Os-isotope records clearly support three major findings. First, the major phase of environmental change during OAE 1a (the "Selli" level; c.f. Coccioni et al., 1987) coincided with almost mantle-like $^{187}Os/^{188}Os_{(i)}$ ratios of ~0.15–0.2 (Bottini et al., 2012). These unradiogenic values must have been maintained for almost 900,000 years by the continual hydrothermal weathering of very large quantities of mafic and ultramafic rocks during a major phase of submarine LIP emplacement. Second, the $^{187}Os/^{188}Os_{(i)}$ records bear some similarity to events surrounding Late Cretaceous OAE 2 because the influence of LIP weathering on ocean chemistry began prior to the onset of OAE 1a (Bottini et al., 2012). This lead-lag relationship implies a causal relationship between the O-J LIP and major environmental change during OAE 1a. Somewhat enigmatic, less radiogenic $^{187}Os/^{188}Os_{(i)}$ ratios in Upper Barremian strata of the Cismon core, Italy, hint at an even earlier, less-intense phase of volcanism that may have been linked to a biocalcification crisis in nannofossil flora (Erba et al., 2010; Bottini et al., 2012). The existing data resolution is, however, not sufficient to resolve this hypothesis. Third, $^{187}Os/^{188}Os_{(i)}$ ratios exhibit significant

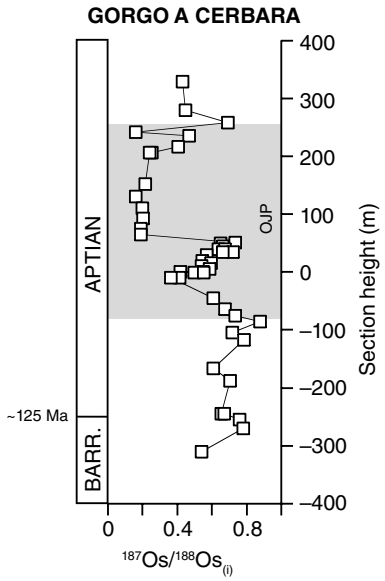

Figure 10.7 Early Cretaceous Os-isotope data spanning part of the emplacement of the Ontong-Java Plateau LIP and Oceanic Anoxic Event 1a. Data are from Tejada et al. (2009). The grey-shaded region denotes a shift toward more unradiogenic seawater $^{187}Os/^{188}Os$ ratios that are taken to record the rapid weathering of basalts associated with LIP emplacement and/or a reduction in the weathering rate of continental rocks.

shifts throughout OAE 1a, with radiogenic values occurring at the base of the Selli level at Gorgo a Cerbara (Italy; Tejada et al., 2009) and Cismon (Bottini et al., 2012). As with all $^{187}Os/^{188}Os_{(i)}$ records, such shifts cannot be uniquely interpreted as a reflection of continental weathering because of the interplay between the weathering of *both* mafic and continental rocks. Circumstantial reasoning based on coeval proxy data, however, can assist with qualitative interpretations of such stratigraphic fluctuations in $^{187}Os/^{188}Os_{(i)}$.

10.3.7. The Karoo-Ferrar LIP (189–178 Ma)

Volcanism in the Karoo and Ferrar (K-F) provinces, in present-day South Africa, South America, and Antarctica, has been linked to episodes of rapid environmental change in the Early Toarcian, particularly the Toarcian Oceanic Anoxic Event (T-OAE). Radiometric dating of rocks attributable to the Karoo and Ferrar provinces indicate an overall duration of several millions of years (e.g., Duncan et al., 1997; Sell et al., 2014), with a much shorter period of intense activity around the T-OAE itself, including hydrothermal venting, at ~183 Ma (e.g., Svensen et al., 2007, 2012; Burgess et al., 2015). Three marine $Os_{(i)}$ isotope records span part of the duration of the K-F LIP, from Yorkshire, UK (Cohen et al., 2004); North Wales, UK (Percival et al., 2016); and western Canada (Them et al., 2017). A fourth Os-isotope data set was recently measured in lacustrine shales, of the Chinese D'hanzhai member, which contain distinctly more radiogenic values than the marine sections (Xu et al., 2017). The marine records all retain a similar range of values, which point to a well-mixed ocean inventory of Os in the early Jurassic (Fig. 10.8). They also all exhibit large increases in $^{187}Os/^{188}Os_{(i)}$ ratios toward radiogenic values across the T-OAE in the range 0.3 to 0.8 (Fig. 10.8), which is somewhat counterintuitive given the intense volcanic activity that took place at that time. The explanation for this trend may lie partly in the largely subaerial nature of the K-F LIP and the associated lack of continental breakup, which inhibited the weathering rate of mafic rocks into the oceans following emplacement (Percival et al., 2016). Also, volcanic-driven climate warming probably contributed to the intense weathering of continental crust that would have caused a large influx of radiogenic Os to the oceans, thereby overwhelming any unradiogenic flux (Cohen et al., 2004). The Os isotope records spanning part of the K-F LIP clearly demonstrate the unique characteristics of the climatic and weathering feedbacks associated with this LIP, certainly in contrast with large LIP events of the Cretaceous (Ontong-Java and Caribbean LIPs) (Figs. 10.6 and 10.7). However, no single Os isotope record has yet been produced that spans the entire estimated K-F duration. Establishing such records in the future will be useful to test hypotheses linking volcanism to early Jurassic climate change, particularly in light of recent studies that tend to suggest ocean deoxygenation began considerably earlier than the T-OAE, closer to the putative onset of K-F volcanism before ~183 Ma (Them et al., 2018).

10.3.8. The Central Atlantic Magmatic Province (201.6–200.9 Ma)

The Central Atlantic Magmatic Province (CAMP) has been the subject of many detailed studies that have established precise chronologies of volcanic pulses from ~201.6 to 200.9 Ma (e.g., Schoene et al., 2010; Blackburn et al., 2013; Davies et al., 2017). These, and other stratigraphic studies, have shown a close temporal relationship between initial pulses of intrusive volcanism, a first-order mass extinction, and a large negative carbon isotope excursion of only a few tens of kyrs duration (Hesselbo et al., 2002; Ruhl et al., 2010; Whiteside et al., 2010). While there are two $Os_{(i)}$ isotope records that span the duration of the CAMP, from the southwest UK (Cohen & Coe, 2002) and from Japan (Kuroda et al., 2010), neither of these is presently able to resolve the impact of the CAMP on seawater chemistry with comparable temporal precision to U-Pb chronologies (e.g., Blackburn et al., 2013) or chemostratigraphic studies (e.g., Hesselbo et al., 2002;

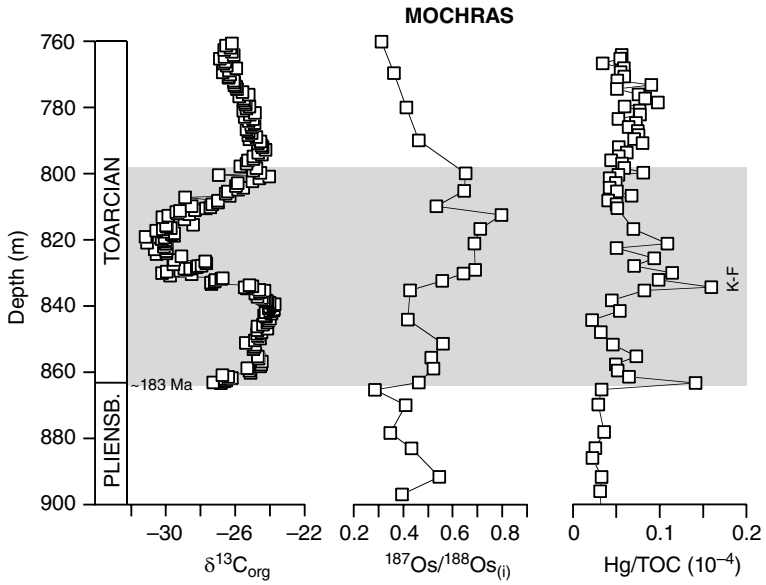

Figure 10.8 Pliensbachian-Toarcian (Early Jurassic) Os-isotope and Hg concentration data spanning the emplacement of the Karoo-Ferrar LIP and the Toarcian Oceanic Anoxic Event. C-isotope data are from Xu et al. (2018), and Os-isotope and Hg concentration data are from Percival et al. (2016). The grey-shaded region denotes the main phase of emplacement of the Karoo-Ferrar LIP.

Ruhl et al., 2011). Both Os records contain evidence for a decrease in the $^{187}Os/^{188}Os$ ratio of seawater between the latest Triassic (Rhaetian) and the early Jurassic (Hettangian) broadly from ~0.3–0.6 to 0.1–0.5. However, the UK record has no data from the critical interval encompassing the earliest emplacement of intrusive magmas and the end-Triassic mass extinction, corresponding to the upper Westbury and Lilstock Formations (Cohen & Coe, 2002) (Fig. 10.9). The Japanese record, in contrast, has a higher stratigraphic resolution, but differs from the UK record in two respects: first, minimum $^{187}Os/^{188}Os_{(i)}$ ratios of ~0.2 occur in late Triassic deposits in Japan, but in early Jurassic deposits in the UK; and second, $^{187}Os/^{188}Os_{(i)}$ ratios are slightly more radiogenic throughout the Japanese section than in the UK. The stratigraphic differences between the sections may be due to the difficulty of correlating the Japanese locality with the northern European biostratigraphic scheme (Kuroda et al., 2010), or to heterogeneity in late Triassic–early Jurassic seawater $^{187}Os/^{188}Os$ ratios. As with the K-F LIP, the potential for Os-isotope chemostratigraphy to unravel the impact of the CAMP on global seawater chemistry at a resolution comparable to the U-Pb geochronology has not yet been fully realized.

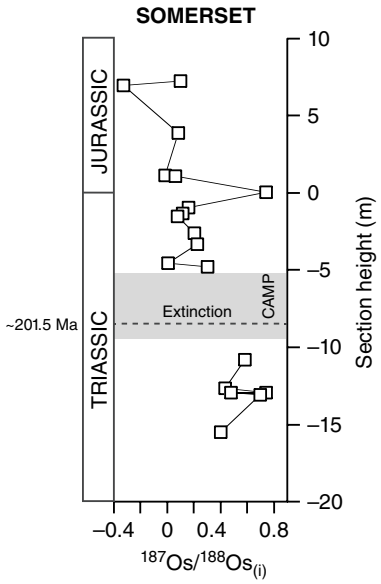

Figure 10.9 Triassic-Jurassic Os-isotope data spanning the emplacement of the Central Atlantic Magmatic Province and the end-Triassic extinction event. Data are from Cohen and Coe (2002). The grey-shaded region denotes the main period of CAMP emplacement. Note that the existing Somerset Os-isotope record does not contain data from within this zone.

10.3.9. The Siberian Traps (~252.2–250.2 Ma)

Zircon U-Pb ages of the Siberian Traps have been used to formulate a model of LIP evolution in relation to the largest mass extinction event of the Phanerozoic Eon. Volcanism began at ~252.4 Ma and ended before ~250.2 ± 0.3 Ma (Kamo et al., 2003; Bowring et al., 1998; Burgess & Bowring, 2015, Burgess et al., 2015, 2017). The mass extinction horizon itself has been tied closely to the first

evidence for intrusive volcanism at ~ 251.9 Ma (Burgess et al., 2017). Despite the detailed chronological constraints on the Siberian Traps, osmium isotope stratigraphy has not yet been applied to this event in great detail. $^{187}Os/^{188}Os_{(i)}$ values have been estimated from Re-Os isochrons with ages of ~252–252.5 Ma, to the range of 0.56 to 0.62 (Georgiev et al., 2011) (Fig. 10.10). These data tend to suggest a limited evolution of seawater $^{187}Os/^{188}Os$ across the early interval of volcanism, although younger Re-Os data sets (247–234 Ma) have $^{187}Os/^{188}Os_{(i)}$ values of ~0.8–1.4, implying a slight evolution of seawater to more radiogenic values by the early Triassic (Yang et al., 2004; Xu et al., 2009; Pašava et al., 2009). Nonetheless, the data are of low resolution and do not clearly cover the major phase of intrusive volcanism, allowing for the large uncertainties in the Re-Os estimates of depositional ages and $^{187}Os/^{188}Os_{(i)}$ (Georgiev et al., 2011). A single stratigraphic record at Opal Creek, Alberta, exhibits a decrease in $^{187}Os/^{188}Os_{(i)}$ from 0.54 to 0.35 following the Late Permian extinction level, followed by a return to ~0.60 at the Permian-Triassic boundary (Schoepfer et al., 2012) (Fig. 10.10). These data suggest a transient excursion in seawater Os chemistry toward unradiogenic $^{187}Os/^{188}Os$ values during an interval of intrusive volcanism in the Siberian Traps (c.f. Burgess et al., 2017), which is temporally constrained by U-Pb ages to a duration <60 kyrs (c.f. Burgess et al., 2014).

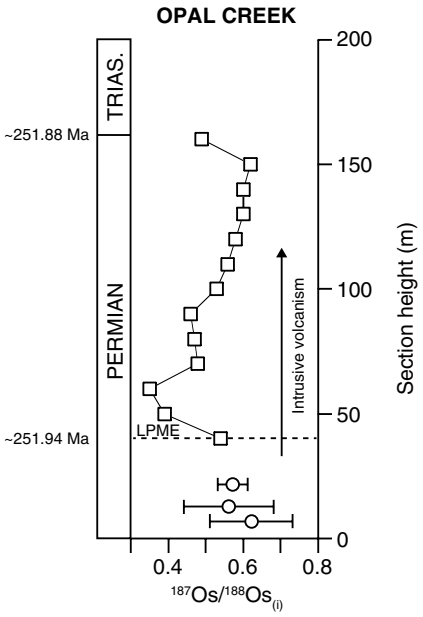

Figure 10.10 End-Permian Os-isotope data spanning the emplacement of the Siberian Traps LIP. Circles for the Siberian Traps are for three $^{187}Os/^{188}Os_{(i)}$ estimates (Georgiev et al., 2011) whose age uncertainties span the entire duration of LIP emplacement (c.f. Burgess & Bowring, 2014). Additional data (squares) are from Schoepfer et al. (2012).

Additional data for this section show a small excursion to an unradiogenic value of ~0.20 shortly following the main extinction level (Georgiev et al., 2015). The reasons for this brief excursion are not clear but may be linked to variations in subaerial basalt weathering and/or the transport of radiogenic or unradiogenic weathering signals from the Siberian LIP to the global ocean. The relatively small magnitude of documented $^{187}Os/^{188}Os_{(i)}$ variation for the Siberian Traps, compared with, for example, the CAMP or OJP LIPs, may be related to the high latitude of their emplacement, which would have resulted in a low weathering rate. Thus, the impact of the Siberian Traps on ocean Os chemistry may have been disproportionate to their considerable environmental impact.

10.4. SUMMARY: OS-ISOTOPE STRATIGRAPHY AND LIPS

Os isotope data from a number of marine sedimentary successions have been instrumental in establishing the link between LIP volcanism and major environmental changes in the Early Cretaceous (OAE 1a) and Late Cretaceous (OAE 2), with significant shifts in seawater chemistry to mantle-like values over timescales of 10^4–10^5 years (Turgeon & Creaser, 2008; Tejada et al., 2009; Bottini et al., 2012; Du Vivier et al., 2014, 2015). The data have been useful in distinguishing the effect of extraterrestrial impacts and LIP volcanism on major extinction events (Ravizza & Peucker-Ehrenbrink, 2003; Robinson et al., 2009) and in testing hypotheses of Earth-system feedbacks during LIP-inspired intervals of profound global warming (Cohen et al., 2004; Dickson et al., 2015; Percival et al., 2016; Them et al., 2017).

Nonetheless, the usefulness of Os-isotope stratigraphy to understand the timing and effects of LIP volcanism is capable of further refinement. Os isotopes have most commonly been used to investigate the effects of volcanism on stratigraphically well-defined episodes of environmental change, thus testing putative links between volcanism and climate. While these groundbreaking studies established the fundamental basis for this approach, the resulting data do not often span the full interval of LIP activity. Additionally, the fundamental drivers of the Os-isotope budget of the oceans (the weathering of continental and oceanic rocks) make it difficult to uniquely disentangle the effects of basalt and continental rock weathering on seawater $^{187}Os/^{188}Os$ ratios. Many different factors may cause the balance of the weathering products of these sources to vary over time, in addition to the simple presence of a LIP. Such factors include the prevalence of intrusive or extrusive volcanism; the amount and composition of Os liberated from igneous and sedimentary rocks during intrusive events; the latitude of LIP

emplacement (and thus proximity to regions of intense physical or chemical weathering); the association of LIP emplacement with continental breakup (i.e., the CAMP); and the effects of volcanism-climate feedbacks on the intensity and/or congruency of global weathering regimes. The heterogeneous Os isotope signatures of Phanerozoic LIPs reflect the many ways in which these factors can combine in both time and space.

The recent emergence of mercury (Hg) concentrations as a proxy for volcanism (e.g., Sanei et al., 2012; Percival et al., 2015; Charbonnier et al., 2017; Scaife et al., 2017; Percival et al., Chapter 11 this volume) opens the possibility of pairing Os-isotopes with Hg analyses to help interpret stratigraphic variations in $^{187}Os/^{188}Os_{(i)}$ (e.g., Percival et al., 2016) (Fig. 10.8). Additionally, the role of continental rock weathering as a driver of Os-isotope change in the oceans might also be better constrained by pairing these measurements with other emerging proxies for silicate weathering, such as Li isotopes. One such application of Os and Li isotopes, to OAE 2, has been used to calculate the mass of basalts weathered into the oceans during that event (Pogge van Strandmann et al., 2013). Paired applications of Os and Li may yield fruitful insights into global weathering patterns related to other LIP events.

Os-isotope stratigraphy holds a crucial place in the compendium of approaches used to investigate the effect of LIPs on the Earth's environment. Future applications of this technique at even finer temporal scales will offer further insights into the timing and environmental consequences of LIPs.

ACKNOWLEDGMENTS

This work was supported by Natural Environmental Research Council standard grant NE/F021313/1.

REFERENCES

Adams, D. D., Hurtgen, M. T., & Sageman, B. B. (2010). Volcanic triggering of a biogeochemical cascade during Oceanic Anoxic Event 2. *Nature Geoscience, 3,* 201–204.

Allègre, C. J., Birck, J. L., Capmas, F., & Courtillot, V. (1999). Age of the Deccan traps using ^{187}Re-^{187}Os systematics. *Earth & Planetary Science Letters, 170,* 197–204.

Barry, T. L., Kelley, S. P., Reidel, S. P., Camp, V. E., Self, S., Jarboe, N. A., Duncan, R. A., et al. (2013). *Eruption chronology of the Columbia River Basalt Group*. Geological Society of America Special Paper *497*, 45–66.

Blackburn, T. J., Olsen, P. E., Bowring, S. A., Kent, D. V., Puffer, J., McHone, G., Rasbury, E. T., et al. (2013). Zircon U-Pb geochronology links the end-Triassic extinction with the Central Atlantic Magmatic Province. *Science, 340,* 941–945.

Bottini, C., Cohen, A. S., Erba, E., Jenkyns, H., & Coe, A. L. (2012) Osmium-isotope evidence for volcanism, weathering and ocean mixing during early Aptian OAE 1a. *Geology, 40,* 583–586.

Bowring, S. A., Erwin, D. H., Jin, Y. G., Martin, M. W., Davidek, K., & Wang, W. (1998). U/Pb zircon geochronology and tempo of the end-Permian mass extinction. *Science, 280,* 1039–1045.

Brinkhuis, H., Schouten, S., Collinson, M. E., Sluijs, A., Sinninghe Damsté, J. S., Dickens, G. R., Huber, M., et al. (2006). Episodic fresh surface waters in the Eocene Arctic Ocean. *Nature, 441,* 606–609.

Burgess, S. D., & Bowring, S. A. (2015). High-precision geochronology confirms voluminous Magmatism before, during and after Earth's most severe extinction. *Science Advances, 1,* e1500470.

Burgess, S. D., Bowring, S., & Shen, S. (2014). High-precision timeline for Earth's most severe extinction. *Proceedings of the National Academy of Sciences of the United States of America, 111,* 3316–3321.

Burgess, S. D., Bowring, S. A., Fleming, T. H., & Elliot, D. H. (2015). High-precision geochronology links the Ferrar large igneous province with early-Jurassic ocean anoxia and biotic crisis. *Earth and Planetary Science Letters, 415,* 90–99.

Burgess, S. D., Muirhead, J. D., & Bowring, S. A. (2017). Initial pulse of Siberian Traps sills as the trigger of the end-Permian mass extinction. *Nature Communications, 8,* 164.

Burton, K. W. (2006). Global weathering variations inferred from marine radiogenic isotope records. *Journal of Geochemical Exploration, 88,* 262–265.

Burton, K. W., Bourdon, B., Birck, J-L., Allègre, C. J., & Hein, J. R. (1999). Osmium isotope variations in the oceans recorded by Fe-Mn crusts. *Earth and Planetary Science Letters, 171,* 185–197.

Charbonnier, G., Morales, C., Duchamp-Alphonse, S., Westermann, S., Adatte, T., & Föllmi, K. B. (2017). Mercury enrichment indicates volcanic triggering of Valanginian environmental change. *Scientific Reports, 7,* 40808.

Chenet, A. L., Quidelleur, X., Fluteau, F., & Courtillot, V. (2007). ^{40}K-^{40}Ar dating of the main Deccan large igneous province: further evidence of KTB age and short duration. *Earth and Planetary Science Letters, 263,* 1–15.

Coccioni, R., Nesci, O., Tramontana, M., Wezel, F. C., & Moretti, E. (1987). Descrizione di un livello-guida "radiolaritico-bituminoso-ittiolitico" alla base delle Marne a Fucoidi nell'Appennino umbro-marchigiano. *Bollettino-Societa Geologica Italiana, 106,* 183–192.

Cohen, A. S., & Coe, A. L. (2002). New geochemical evidence for the onset of volcanism in the Central Atlantic magmatic province and environmental change at the Triassic-Jurassic boundary. *Geology, 30,* 267–270.

Cohen, A. S., Coe, A. L., Bartlett, J. M., & Hawksworth, C. J. (1999). Precise Re-Os ages of organic-rich mudrocks and the Os-isotope composition of Jurassic seawater. *Earth and Planetary Science Letters, 167,* 159–173.

Cohen, A. S., Coe, A. L., Harding, S. M., & Schwark, L. (2004). Osmium isotope evidence for the regulation of atmospheric CO_2 by continental weathering. *Geology, 32,* 157–160.

Coffin, M. F., & Eldholm, O. (1992). Volcanism and continental break-up: a global compilation of large igneous provinces. In B. C. Storey, T. Alabaster, & R. J. Pankhurst (Eds.),

Magmatism and the causes of continental break-up. *Geological Society of London Special Publication, 68,* 21–34.

Coffin, M. F., & Eldholm, O. (1994). Large igneous provinces: Crustal structure, dimensions, and external consequences. *Reviews of Geophysics, 32,* 1–36.

Courtillot, V. E., & Renne, P. R. (2003). On the ages of flood basalt events. *Comptes rendus Geoscience, 335,* 113–140.

Cucciniello, C., Langone, A., Melluso, L., Morra, V., Mahoney, J. J., Meisel, T., & Tiepolo, M. (2010). U-Pb ages, Pb-Os isotope ratios, and platinum group element (PGE) compositions of the West Central Madagascar Flood Basalt Province. *Journal of Geology, 118,* 523–541.

Davies, J. H. F. L., Marzoli, A., Bertrand, H., Youbi, N., Ernesto, M., & Schaltegger, U. (2017). End-Triassic mass extinction started by intrusive CAMP activity. *Nature Communications, 8,* 15596.

Dickson, A. J., & Cohen, A. S. (2012). A molybdenum isotope record of Eocene Thermal Maximum 2: implication for global ocean redox during the early Eocene. *Paleoceanography and Paleoclimatology, 27*. doi:10.1029/2012PA002346

Dickson, A. J., Cohen, A. S., Coe, A. L., Davies, M., Shcherbinina, E. A., & Gavrilov, Y. (2015). Evidence for weathering and volcanism during the PETM from Arctic Ocean and Peri-Tethys osmium isotope records. *Palaeogeography, Palaeoclimatology, Palaeoecology, 438,* 300–307.

Duncan, R. A. (2002). A time frame for construction of the Kerguelen Plateau and Broken Ridge. *Journal of Petrology, 43,* 1109–1119.

Duncan, R. A., Hooper, P. R., Rehacek, J., Marsh, J. S., & Duncan, A. R. (1997). The timing and duration of the Karoo igneous event, southern Gondwana. *Journal of Geophysical Research*, *102,* 18127–18138.

Du Vivier, A. D. C., Selby, D., Condon, D. J., Takashima, R., & Nishi, H. (2015). Pacific $^{187}Os/^{188}Os$ isotope chemistry and U-Pb geochronology: Synchoneity of global Os isotope change across OAE 2. *Earth and Planetary Science Letters, 428,* 204–216.

Du Vivier, A. D. C., Selby, D., Sageman, B. B., Jarvis, I., Gröcke, D. R., , & Voigt, S. (2014). Marine $^{187}Os/^{188}Os$ isotope stratigraphy reveals the interaction of volcanism and ocean circulation during Oceanic Anoxic Event 2. *Earth and Planetary Science Letters, 389,* 23–33.

Eldrett, J. S., Dodsworth, P., Bergman, S. C., Wright, M., & Minisini, D. (2017). Water-mass evolution in the Cretaceous Western Interior Seaway of North American and equatorial Atlantic. *Climate of the Past, 13,* 855–878.

Eldrett J. S., Minisini D., & Bergman S. C. (2014). Decoupling of the carbon cycle during Ocean Anoxic Event 2. *Geology, 42*(7), 567–570.

Erba, E., Bottini, C., Weissert, H. J., & Keller, C. E. (2010). Calcareous nannoplankton response to surface-water acidification around Oceanic Anoxic Event 1a. *Science, 329,* 428–432.

Erbacher, J., Friedrich, O., Wilson, P. A., Birch, H., & Mutterlose, J. (2005). Stable organic carbon isotope stratigraphy across Oceanic Anoxic Event 2 of Demerara Rise, western tropical Atlantic. *Geochemistry, Geophysics, Geosystems, 6,* Q06010. doi:10.1029/2004GC000850

Ernst, R. (2014). Large Igneous Provinces. Cambridge: Cambridge University Press.

Ernst, R., & Youbi, N. (2017). How large igneous provinces affect global climate, sometimes cause mass extinctions, and represent natural markers in the geological record. *Palaeogeography, Palaeoclimatology, Palaeoecology, 478,* 30–52.

Esser, B. K., & Turekian, K. K. (1989). Osmium isotopic composition of the Raton Basin Cretaceous-Tertiary boundary interval. *EOS, Transactions of the American Geophysical Union, 70,* 717.

Esser, B. K., & Turekian, K. K. (1993). The osmium isotopic composition of the continental crust. *Geochimica et Cosmochimica Acta, 57,* 3093–3104.

Frieling, J., Svensen, H. H., Planke, S., Cramwinkel, M. J., Selnes, H., & Sluijs, A. (2016). Thermogenic methane release as a cause for the long duration of the PETM. *Proceedings of the National Academy of Sciences of the United States of America, 113,* 12059–12064.

Geissbühler, M. (1990). Bestimmung von Osmium Isotopenverhältnissen in Sedimenten der Kreide-Tertiär-Grenze und in Aerosolen aus Mantelvulkanen von Hawaii mittels SIMS. Ph.D. thesis, Bern, Switzerland, Universität Bern.

Georgiev, S., Stein, H. J., Hannah, J. L., Bingen, B., Weiss, H. M., & Piasecki, S. (2011). Hot acidic late Permian seas stifle life in record time. *Earth and Planetary Science Letters, 310,*389–400.

Georgiev, S. V., Stein, H. J., Hannah, J. L., Henderson, C. M., & Algeo, T. J. (2015). Enhanced recycling of organic matter and Os-isotope evidence for multiple magmatic or meteoric inputs to the Late Permian Panthalassic Ocean, Opal Creek, Canada. *Geochimica et Cosmochimica Acta, 150,* 192–210.

Hesselbo, S. P., Robinson, S. A., Surlyk, F., & Piasecki, S. (2002). Terrestrial and marine extinction at the Triassic-Jurassic boundary synchronized with major carbon-cycle perturbation: a link to initiation of massive volcanism? *Geology, 30,* 251–254.

Hofmann, C., Courtillot, V., Féraud, G., Rochette, P., Yirgus, G., Ketefo, E., & Pik, R. (1997). Timing of the Ethiopian flood basalt event and implications for plume birth and global change. *Nature, 389,* 838–841.

Holmden, C., Jacobson, A. D., Sageman, B. B., & Hurtgen, M. T. (2016). Response of the Cr isotope proxy to Cretaceous Ocean Anoxic Event 2 in a pelagic carbonate succession from the Western Interior Seaway. *Geochimica et Cosmochimica Acta, 186,* 277–295.

Jenkyns, H. C. (2010). Geochemistry of Oceanic Anoxic Event. *Geochemistry Geophysics Geosystems, 11*. doi: 10.1029/2009GC002788

Jones, M. T., Percival, L. M. E., Stokke, E. W., Frieling, J., Mather, T. A. Riber, L., Schubert, B. A., et al. (2019). Mercury anomalies across the Palaeocene-Eocene Thermal Maximum. *Climate of the Past, 15,* 217–236.

Kamo, S. L., Czamanske, G. K., Amelin, Y., Fedorenko, V. A., Davis, D. W., & Trofimov, V. R. (2003). Rapid eruption of Siberian flood-volcanic rocks and evidence for coincidence with the Permian–Triassic boundary. *Earth and Planetary Science Letters, 214*, 75–91.

Kasbohm, J., & Schoene, B. (2018). Rapid eruption of the Columbia River flood basalt and correlation with the mid-Miocene climate optimum. *Science Advances, 4,* eaat8223.

Kingsbury, C. G., Kamo, S. L., Ernst, R. E., Söderlund, U., & Cousens, B. L. (2018). U-Pb geochronology of the plumbing system associated with the Late Cretaceous Strand Fiord Formation, Axel Heiberg Island, Canada: part of the 130–90 Ma High Arctic large igneous province. *Journal of Geodynamics, 118,* 106–117.

Klemm, V., Frank, M., Levasseur, S., Halliday, A. N., & Hein, J. R. (2008). Seawater osmium isotope evidence for a middle Miocene flood basalt event in ferromanganese crusts. *Earth and Planetary Science Letters, 273,* 175–183.

Klemm, V., Levasseur, S., Frank, M., Hein, J. R., & Halliday, A. N. (2005) Osmium isotope stratigraphy of a marine ferromanganese crust. *Earth and Planetary Science Letters, 238,* 42–48.

Kuroda, J., Hori, R. S., Suzuki, K., Gröcke, D. R., & Ohkouchi, N. (2010). Marine osmium isotope record across the Triassic-Jurassic boundary from a Pacific pelagic site. *Geology, 38,* 1095–1098.

Kuroda, J., Ogawa, N. O., Tanimizu, M., Coffin, M. F., Tokuyama, H., Kitazato, H., & Ohkouchi, N. (2007). Contemporaneous massive subaerial volcanism and late Cretaceous Oceanic Anoxic Event 2. *Earth and Planetary Science Letters, 256,* 211–223.

Levasseur, S., Birck, J-L., & Allègre, C. J. (1998). Direct measurement of femtomoles of osmium and the $^{187}Os/^{186}Os$ ratio in seawater. *Science, 282,* 272–274;Levasseur, S., Birck, J-L., & Allègre, C. J. (1999). The osmium riverine flux and the oceanic mass balance of osmium. *Earth and Planetary Science Letters, 174,* 7–23.

Loewen, M. W., Duncan, R. A., Kent, A. J. R., & Krawl, K. (2013). Prolonged plume volcanism in the Caribbean Large Igneous Province: new insights from Curaçao and Haiti. *Geochemistry, Geophysics, Geosystems, 14,* 4241–4259.

Luck, J-M., & Allègre, C. J. (1983). ^{187}Re-^{187}Os systematics in meteorites and cosmochemical consequences. *Nature, 302,* 130–132.

Luck, J-M., Birck, J-L., & Allègre, C. J. (1980). ^{187}Re-^{187}Os systematics in meteorites: Early chronology of the solar system and the age of the galaxy. *Nature*, *283,* 256–259.

Malinverno, A., Erba, E., & Herbert, T. D. (2010). Orbital tuning as an inverse problem: chronology of the early Aptian oceanic anoxic event 1a (Selli level) in the Cismon APTICORE. *Paleoceanography and Paleoclimatology, 25*. doi:10.1029/2009PA001769

Meisel, T., Krähenbühl, U., & Nazarov, M. A. (1995). Combined osmium and strontium isotopic study of the Cretaceous-Tertiary boundary at Sumbar, Turkmenistan: A test for an impact vs. a volcanic hypothesis. *Geology, 23,* 313–316.

Meyers, S. R., Siewert, S. E., Singer, B. S., Sageman, B. B., Condon, D. J., Obradovich, J. D., Jicha, B. R., et al. (2012). Intercalibration of radioisotopic and astrochronologic time scales for the Cenomanian-Turonian boundary interval, Western Interior Basin, USA. *Geology, 40,* 7–10.

Orth, C. J., Attrep, M. Jr., Quintana, L. R., Elder, W. P., Kauffman, E. G., Diner, R., & Vilamil, T. (1993). Elemental abundance anomalies in the late Cenomanian extinction interval: A search for the source(s). *Earth and Planetary Science Letters, 117,* 189–204.

Pašava, J., Oszczepalski, S., & Du, A. D. (2009). Re-Os age of non-mineralized black shale from the Kupferschiefer, Poland, and implications for metal enrichment. *Mineralium Deposita, 45,* 189–199.

Pegram, W. J., & Turekian, K. K. (1999). The osmium isotopic composition of Cenozoic sea water as inferred from a deep-sea core corrected for meteoric contributions. *Geochimica et Cosmochimica Acta, 63,* 4053–4058.

Pegram, W. J., Esser, B. K., Krishnaswami, S., & Turekian, K. K. (1994). The isotopic composition of leachable osmium from river sediments. *Earth and Planetary Science Letters, 128,* 591–599.

Pegram, W. J., Krishnaswami, S., Ravizza, G. E., & Turekian, K. K. (1992). The record of sea water 187Os/186Os variation through the Cenozoic. *Earth and Planetary Science Letters, 113,* 569–576.

Percival, L. M. E., Cohen, A. S., Davies, M. K., Dickson, A. J., Hesselbo, S. P., Jenkyns, H. C., Leng, M. J., et al. (2016). Osmium isotope evidence for two pulses of increased continental weathering linked to Early Jurassic volcanism and climate change. *Geology, 44,* 759–762.

Percival, L. M. E., Witt, M. L. I., Mather, T. A., Hermoso, M., Jenkyns, H. C., Hesselbo, S. P., Al-Suwaidi, A. H., et al. (2015). Globally enhanced mercury deposition during the end-Pliensbachian and Toarcian OAE: A link to the Karoo-Ferrar Large Igneous Province. *Earth and Planetary Science Letters, 428,* 267–280.

Peucker-Ehrenbrink, B., & Jahn, B. M. (2001) Rhenium-osmium isotope systematics and platinum-group elements concentrations: loess and the upper continental crust. *Geochemistry Geophysics Geosystems, 2,* 1061. doi:10.1029/2001GC000172

Peucker-Ehrenbrink, B., & Ravizza, G. (2000) The marine osmium isotope record. *Terra Nova, 12,* 205–219.

Peucker-Ehrenbrink, B., & Ravizza, R. (2012). Osmium isotope stratigraphy. In F. Gradstein, J. Ogg, M. Schmitz, & G. Ogg (Eds.), *The Geologic Time Scale 2012*. Elsevier.

Peucker-Ehrenbrink, B., Ravizza, G., & Hofmann, A. W. (1995). The marine $^{187}Os/^{186}Os$ record of the past 80 million years. *Earth and Planetary Science Letters, 130,* 155–167.

Pogge von Strandmann, P. A. E., Jenkyns, H. C., & Woodfine, R. G. (2013). Lithium isotope evidence for enhanced weathering during Oceanic Anoxic Event 2. *Nature Geoscience, 6*, 668–672.

Prokoph, A., El Bilali, H., & Ernst, R. (2013). Periodicities in the emplacement of large igneous provinces through the Phanerozoic: Relations to ocean chemistry and marine biodiversity evolution. *Geoscience Frontiers, 4,* 263–276.

Ravizza, G. (2007). Reconstructing the marine $^{187}Os/^{188}Os$ record and the particulate flux of meteoric osmium during the late Cretaceous. *Geochimica et Cosmochimica Acta, 71,* 1355–1369.

Ravizza, G., & Peucker-Ehrenbrink, B. (2003). Chemostratigraphic evidence of Deccan volcanism from the marine osmium isotope record. *Science, 302,* 1392–1395.

Ravizza, G., & Turekian, K. K. (1989). Application of the ^{187}Re-^{187}Os system to back shale geochronometry. *Geochimica et Cosmochimica Acta, 53*, 3257–3262.

Ravizza, G., & Turekian, K. K. (1992). The osmium isotope composition of organic-rich marine sediments. *Earth and Planetary Science Letters, 110*, 1–6.

Ravizza, G., Norris, R. N., Blusztajn, J., & Aubry, M-P. (2001) An osmium isotope excursion associated with the late Paleocene Thermal Maximum: Evidence of intensified chemical weathering. *Paleoceanography, 16,* 155–163.

Riedel, S. P., Camp, V. E., Tolan, T. L., & Martin, B. S. (2013). The Columbia River flood basalt province: stratigraphy, areal extent, volume and physical volcanology. *Geological Society of America Special Paper, 497,* 1–43.

Robinson, N., Ravizza, G., Coccioni, R., Peucker-Ehrenbrink, B., & Norris, R. (2009). A high-resolution marine $^{187}Os/^{188}Os$ record for the late Maastrichtian: distinguishing the chemical fingerprints of Deccan volcanism and the KP impact event. *Earth and Planetary Science Letters, 281*, 159–168.

Robinson, S. A., Dickson, A. J., Pain, A., Jenkyns, H. C., O'Brien, C. L., Farnsworth, A., & Lunt, D. J. (2019). Southern hemisphere sea-surface temperatures during the Cenomanian–Turonian: Implications for the termination of Oceanic Anoxic Event 2. *Geology.* doi:10.1130/G45842.1

Ruhl, M., Bonis, N. R., Reichart, G-J., Sinninghe Damsté, J. S., & Kürschner, W. M. (2011). Atmospheric carbon injection linked to end-Triassic mass extinction. *Science, 333*, 430–434.

Ruhl, M., Deenen, M. H. L., Abels, H. A., Krijgsman, W., & Kürschner, W. M. (2010). Astronomical constraints on the duration of the early Jurassic Hettangian stage and recovery rates following the end-Triassic mass extinction, St Audrie's Bay, East Quantoxhead, UK. *Earth and Planetary Science Letters, 295*, 262–276.

Sanei, H., Grasby, S., & Beauchamp, B. (2012) Latest Permian mercury anomalies. *Geology, 40,* 63–66.

Sato, H., Onoue, T., Nozaki, T., & Suzuki, K. (2013). Osmium isotope evidence for a large Late Triassic impact event. *Nature Communications, 4,* 2455.

Scaife, J. D., Ruhl, M., Dickson, A. J., Mather, T. A., Jenkyns, H. C., Percival, L. M. E., Hesselbo, S. P., et al. (2017). Sedimentary mercury enrichments as a marker for submarine large igneous province volcanism? Evidence from the mid-Cenomanian Event and Oceanic Anoxic Event 2 (Late Cretaceous). *Geochemistry, Geophysics, Geosystems, 18,* 4253–4275.

Schaller, M. F., Fung, M. K., Wright, J. D., Katz, M. E., & Kent, D. V. (2017). Impact ejecta at the Paleocene-Eocene boundary. *Science, 354*, 225–229.

Schoene, B., Eddy, M. P., Samperton, K. M., Keller, C. B., Keller, G., Adatte, T., & Khadri, S. F. R. (2019). U-Pb constraints on pulsed eruption of the Deccan Traps across the end-Cretaceous mass extinction. *Science, 363,* 862–866.

Schoene, B., Guex, J., Bartoli, A., Schaltegger, U., & Blackburn, T. J. (2010). Correlating the end-Triassic extinction and flood basalt volcanism at the 100 ka level. *Geology, 38,* 387–390.

Schoene, B., Samperton, K. M., Eddy, M. P., Keller, G., Adatte, T., Bowring, S. A., Khadri, S. F. R., & Gertsch, B. (2015). U-Pb geochronology of the Deccan Traps and relation to the end-Cretaceous mass extinction. *Science, 347,* 182–184.

Schoepfer, S. D., Henderson, C. M., Garrison, G. H., Foriel, J., Ward, P. D., Selby, D., Hower, J. C., et al. (2012). Termination of a continent-margin upwelling system at the Permian-Triassic boundary (Opal Creek, Alberta, Canada). *Global and Planetary Change, 105,* 21–35.

Sell, B., Ovtcharova, M., Guex, J., Bartolini, A., Jourdan, F., Spangenberg, J. E, Vicente, J-C., et al. (2014). Evaluating the temporal link between the Karoo LIP and climatic-biotic events of the Toarcian stage with high-precision U-Pb geochronology. *Earth and Planetary Science Letters, 408,* 48–56.

Sharma, M., Papanastassiou, D. A., & Wasserburg, G. J. (1997). The concentration and isotopic composition of osmium in the oceans. *Geochimica et Cosmochimica Acta, 61,* 3287–3299.

Sluijs, A., Schouten, S., Donders, T. H., Schoon, P. L., Röhl, U., Reichart, G-J., Sangiorgi, F., Kim, J-H., et al. (2009). Warm and wet conditions in the Arctic region during Eocene Thermal Maximum 2. *Nature Geoscience, 2,* 777–780.

Storey, M., Duncan, R. A., & Swisher, C. C. III (2007). Paleocene-Eocene Thermal Maximum and the opening of the northeast Atlantic. *Science, 316,* 587–589.

Storey, M., Duncan, R. A., & Tegner, C. (2007b) Timing and duration of volcanism in the North Atlantic Igneous Province: implications for geodynamics and links to the Iceland hotspot. *Chemical Geology, 241,* 264–281.

Svensen, H., Corfu, F., Polteau, S., Hammer, Ø., & Planke, S. (2012). Rapid emplacement in the Karoo Large Igneous Province. *Earth and Planetary Science Letters, 325–326,* 1–9.

Svensen, H., Planke, S., & Corfu, F. (2010). Zircon dating ties NE Atlantic sill emplacement to initial Eocene global warming. *Journal of the Geological Society of London, 167,* 433–436.

Svensen, H., Planke, S., Chevallier, L., Malthe-Sørenssen, A., Corfu, F., & Jamtveit, B. (2007). Hydrothermal venting of greenhouse gases triggering Early Jurassic global warming. *Earth and Planetary Science Letters, 256,* 554–566.

Svensen, H., Planke, S., Malthe-Sørenssen, A., Jamtveit, B., Myklebust, R., Rasmussen Eidem, T., & Rey, S. S. (2004). Release of methane from a volcanic basin as a mechanism for initial Eocene global warming. *Nature, 429,* 542–545.

Tejada, M. L. G., Suzuki, K., Kuroda, J., Coccioni, R., Mahoney, J. J., Ohkouchi, N., Sakamoto, T. et al. (2009). Ontong Java Plateau eruption as a trigger for the early Aptian oceanic anoxic event. *Geology, 37,* 855–858.

Them, T. R., Gill, B. C., Caruthers, A. H., Gerhardt, A. M., Gröcke, D. R., Lyons, T. W., Marroquín, S. M., et al. (2018). Thallium isotopes reveal protracted anoxia during the Toarcian (early Jurassic) associated with volcanism, carbon burial and mass extinction. *Proceedings of the National Academy of Sciences of the United States of America, 115,* 6596–6601.

Them, T. R., Gill, B. C., Selby, D., Gröcke, D. R., Friedman, R. M., & Owens, J. D. (2017). Evidence for rapid weathering response to climatic warming during the Toarcian Oceanic Anoxic event. *Scientific Reports, 7,* 5003.

Thomas, E., & Shackleton, N. J. (1996). The Paleocene-Eocene benthic foraminiferal extinction and stable isotope anomalies. *Geological Society of London Special Publication, 101,* 401–441.

Timm, C., Hoernle, K., Werner, R., Hauff, F., van den Bogaard, P., Michael, P., Coffin, M. F., et al. (2011). Age and geochemistry of the oceanic Manihiki Plateau, SW Pacific: New evidence for a plume origin. *Earth and Planetary Science Letters, 304,* 135–146.

Touchard, Y., Rochette, P., Aubry, M. P., & Michard, A. (2003). High-resolution magnetostratigraphic and biostratigraphic study of Ethiopian traps-related products in Oligocene sediments from the Indian Ocean. *Earth and Planetary Science Letters, 3–4,* 493–508.

Tsikos, H., Jenkyns, H. C., Walsworth-Bell, B., Petrizzo, M. R., Forster, A., Kolonic, S., Erba, E., et al. (2004). Carbon isotope stratigraphy recorded by the Cenomanian-Turonian Oceanic Anoxic Event: Correlation and implications based on three key localities. *Journal of the Geology Society of London, 161,* 711–719.

Turgeon, S. C., & Creaser, R. A. (2008) Cretaceous oceanic anoxic event 2 triggered by a massive magmatic episode. *Nature, 454,* 323–326.

Ukstins, I. A., Renne, P. R., Wolfenden, E., Baker, J., Ayalew, D., & Menzies, M. (2002). Matching conjugate volcanic rifted margins: $^{40}Ar/^{39}Ar$ chrono-stratigraphy of pre- and syn-rift bimodal flood volcanism in Ethiopia and Yemen. *Earth and Planetary Science Letters, 198,* 289–306.

Veizer, J. (1989). Strontium isotopes in seawater through time. *Annual Review of Earth and Planetary Sciences, 17,* 141–167.

Walker, R. J., & Morgan, J. W. (1989). Rhenium-Osmium isotope systematics of carbonaceous chondrites. *Science, 243,* 519–522.

Whiteside, J. H., Olsen, P. E., Eglinton, T., Brookfield, M. E., & Sambrotto, R. N. (2010). Compound-specific carbon isotopes from Earths largest flood basalt eruptions directly linked to the end-Triassic mass extinction. *Proceedings of the National Academy of Sciences of the United States of America, 107,* 6721–6725.

Wieczorek, R., Fantle, M. S., Kump, L. R., & Ravizza, G. (2013) Geochemical evidence for volcanic activity prior to and enhanced terrestrial weathering during the Paleocene Eocene thermal maximum. *Geochimica et Cosmochimica Acta.* doi:10.1016/j.gca.2013.06.005

Wignall, P. B. (2001). Large igneous provinces and mass extinctions. *Earth-Science Reviews, 53,* 1–33.

Wilkinson, C. M., Ganerød, M., Hendriks, B. W. H., & Eide, E. A. (2017). Compilation and appraisal of geochronological data from the North Atlantic Igneous Province. In G. Péron-Pinvidic et al. (Eds.), *The NE Atlantic Region: A reappraisal of crustal structure, tectonostratigraphy and magmatic evolution*. Geological Society, London, Special Publications, *447*, 69–103.

Xu, G., Hannah, J. L., Stein, H. J., Bingen, B., Yang, G., Zimmerman, A., Weitscaht, W., et al. (2009). Re-Os geochronology of Arctic black shales to evaluate the Anisian-Ladnian boundary and global faunal correlations. *Earth and Planetary Science Letters, 288,* 581–587.

Xu, W., Ruhl, M., Jenkyns, H. C., Hesselbo, S. P., Riding, J. B., Selby, D., Naafs, B. D. A., et al. (2017). Carbon sequestration in an expanding lake system during the Toarcian Oceanic Anoxic Event. *Nature Geoscience, 10,* 129–134.

Xu, W., Ruhl, M., Jenkyns, H. C., Leng, M. J., Huggett, J. M., Minisini, D., Ullmann, C. V., et al. (2018). Evolution of the Toarcian (Early Jurassic) carbon-cycle and global climatic controls on local sedimentary processes (Cardigan Bay Basin, UK). *Earth and Planetary Science Letters, 484,* 396–411.

Yang, G., Chen, J. F., Du, A. D., Qu, W. J., & Yu, G. (2004). Re-Os dating of Mo-bearing black shale of the Laoyaling deposit, Tongling, Anhui Province, China. *Chinese Scientific Bulletin, 49,* 1396–1400.

Yin, Q. (1995). Development of N-TIMS technique for Re-Os isotope system and its applications to various geochemical problems. PhD thesis, Mainz, Germany, Max-Planck-Gesellschaft.

Zachos, J. C., Quinn, T. M., & Salamy, K. A. (1996). High-resolution (104 years) deep-sea foraminiferal stable isotope records of the Eocene-Oligocene climate transition. *Paleoceanography, 11,* 251–266.